Fall 10-2-2018

8th Annual Postdoctoral Science Symposium

University of Texas MD Anderson Cancer Center PostDoctoral Association

8TH ANNUAL POSTDOCTORAL SCIENCE SYMPOSIUM

October 2, 2018 | Hickey Auditorium

Abstract Booklet

Organized by the MD Anderson Postdoctoral Association

Sponsored by The University of Texas MD Anderson Cancer Center Office of Postdoctoral Affairs and Development, a unit in the Division of Education and Training

THE UNIVERSITY OF TEXAS
MD Anderson Cancer Center
Making Cancer History®

Mission of the Annual Postdoctoral Science Symposium

To provide a platform for talented postdoctoral fellows throughout the Texas Medical Center to present their work to a wider audience, the MD Anderson Postdoctoral Association convened the inaugural Annual Postdoctoral Science Symposium (APSS) on August 4, 2011.

The APSS provides a professional venue for postdoctoral scientists to develop, clarify, and refine their research as a result of formal reviews and critiques of faculty and other postdoctoral scientists. Additionally, attendees discuss current research on a broad range of subjects while promoting academic interactions and enrichment and developing new collaborations.

Acknowledgements

The MD Anderson Postdoctoral Association Executive Committee extends sincere gratitude to Dr. Peter W.T. Pisters, MD Anderson President, for his support and encouragement of all MD Anderson trainees.

Furthermore, we thank Dr. Diane Bodurka, Vice President of Education, and the Division of Education and Training for their sponsorship of and assistance with this event. We appreciate the effort required to secure the funding necessary to help establish and execute this symposium. The Postdoctoral Association Executive Committee also thanks the MD Anderson Postdoctoral Advisory Committee for their insights, advocacy, and mentorship throughout the year.

We also recognize the contributions of Dr. Victoria McDonnell of the Office of Postdoctoral Affairs and Development as well as Vondalyn Hall and Kameshia Hunt of Graduate Medical Education. Additionally, we thank Martha Skender in the Division of Education and Training for supporting the inception of the APSS 8 years ago and the teams in Strategic Communications, especially Barry Smith for capturing the event in photos and Jeff Flasik for creating professional symposium materials.

We are indebted to the faculty judges for their constructive evaluation of and feedback to our participants. We also thank the postdoctoral fellow judges for their feedback and review of poster and oral presentations.

We thank Drs. Didem Agac, Yiwen Bu, Anca Chelariu-Raicu, Runzhe Chen, Yating Cheng, Hua-Sheng Chio, Chih-Chien Chou, Jezreel Pantaleon Garcia, Irtiza Hasan, Junwei Hou, Lisa Mustachio, Monica Reyes, Kylee Veazey, Youqiong Ye, and Xiaojie Yu for ensuring the integrity of the abstract organization and review processes.

In addition, we thank Fourwaves and its co-founder Dr. Matthieu Chartier for their in-kind sponsorship and support, which enabled us to complete registration, abstract submissions, and booklet assembly online.

Finally, a big thank you to all of the members of the Postdoctoral Association Executive Committee, especially our organizing committee and outgoing chairs, Drs. Rajan Chaudhari and Kylee Veazey, whose hard work, co-leadership and support made this event possible.

2018 APSS Organizing Committee

Dr. Daisy Izaguirre, Chair

Dr. Alessandra Audia, Vice-Chair

Dr. Rajan Chaudhari, Member

Dr. Kylee Veazey, Member

Dr. Lisa Mustachio, Member

Dr. Vrutant Shah, Member

Dr. Shivanand Pudakalakatti, Member

Dr. Robiya Joseph, Member

Dr. Omkara Veeranki, Member

Dr. Anca Chelariu-Raicu, Member

Competition Winners

Of the nearly 80 abstracts submitted, 12 of the submitting postdoctoral fellows were selected for oral presentations in applied science, basic science, and clinical/translational research. Fifty-four postdoctoral fellows presented scientific posters.

Oral Competition – First-Place Winners

Applied Science: *"Identifying smokers at higher risk for relapse: Validation of a neuroimaging-based classification algorithm"*

David Frank, PhD *Mentor: Francesco Versace, PhD*

Basic Science: "*Metastatic tumor cells influence the transcriptomic and positional heterogeneity of cancer-associated fibroblasts"*

Neus Bota Rabassedas, PhD *Mentor: Jonathan M. Kurie, MD*

Clinical/Translational Research: "*Implications for clinical trial design based on host factors and variation of the gut microbiome of complete responders to immune checkpoint blockade and healthy individuals"*

Vancheswaran Gopalakrishnan, PhD *Mentor: Jennifer Wargo, MD*

Poster Competition Winners

1st Hongyin Wang, PhD *Mentor: Ilya Levental, PhD*	Phosphatidylserine (PS) Externalization Facilitates Membrane Vesiculation Through Decreasing Membrane Stiffness
2nd Seemana Bhattacharya, PhD *Mentor: Gautam Borthakur, MD*	Inhibition of Autophagy Kinase ULK1 Combined with Chemotherapy Results in Modulation of Reactive Oxygen Species and DNA Damage Response to Induce Synergistic Cell Death in Acute Myeloid Leukemia
3rd Priyamvada Jayaprakash, PhD *Mentor: Michael Curran, PhD*	Targeted Hypoxia Reduction Restores T Cell Infiltration and Sensitivity to Immunotherapy in Prostate Cancer

Table of Contents

Oral Presentations

Oral presentations were submitted for the following three categories: Applied Science, Basic Research, and Clinical/Translational Research. Each category included four (4) presenters.

Please note that only abstracts of presenters who agreed to have their abstracts published are included.

APPLIED SCIENCE

Conjugation of HOPO to protein and radiolabeling with Zr-89: Comparative stability and biodistribution in normal mice

Bhasker Radaram, Sandun Perera, David Piwnica-Worms, Mian M. Alauddin

Department of Cancer Systems Imaging, The University of Texas MD Anderson Cancer Center, Houston, TX.

Objectives: Zirconium-89 (^{89}Zr) is attractive for use in antibody-based positron emission tomography due to its radiodecay half-life compatible with the biological half-life of antibodies. Physicians have commonly used deferoxamine (DFO) as a chelating agent for this purpose.[1] However, DFO-chelated ^{89}Zr can suffer from *in vivo* stability challenges.[2] A new chelating agent, 3,4,3-(LI-1,2-HOPO) (HOPO), has demonstrated efficient binding of ^{89}Zr with high stability.[3] We have synthesized three analogs of HOPO exhibiting high *in vitro* and *in vivo* stability with ^{89}Zr. We present conjugation of HOPO to protein, radiolabeling with ^{89}Zr, stability of the labeled protein conjugates, and their biodistribution results.

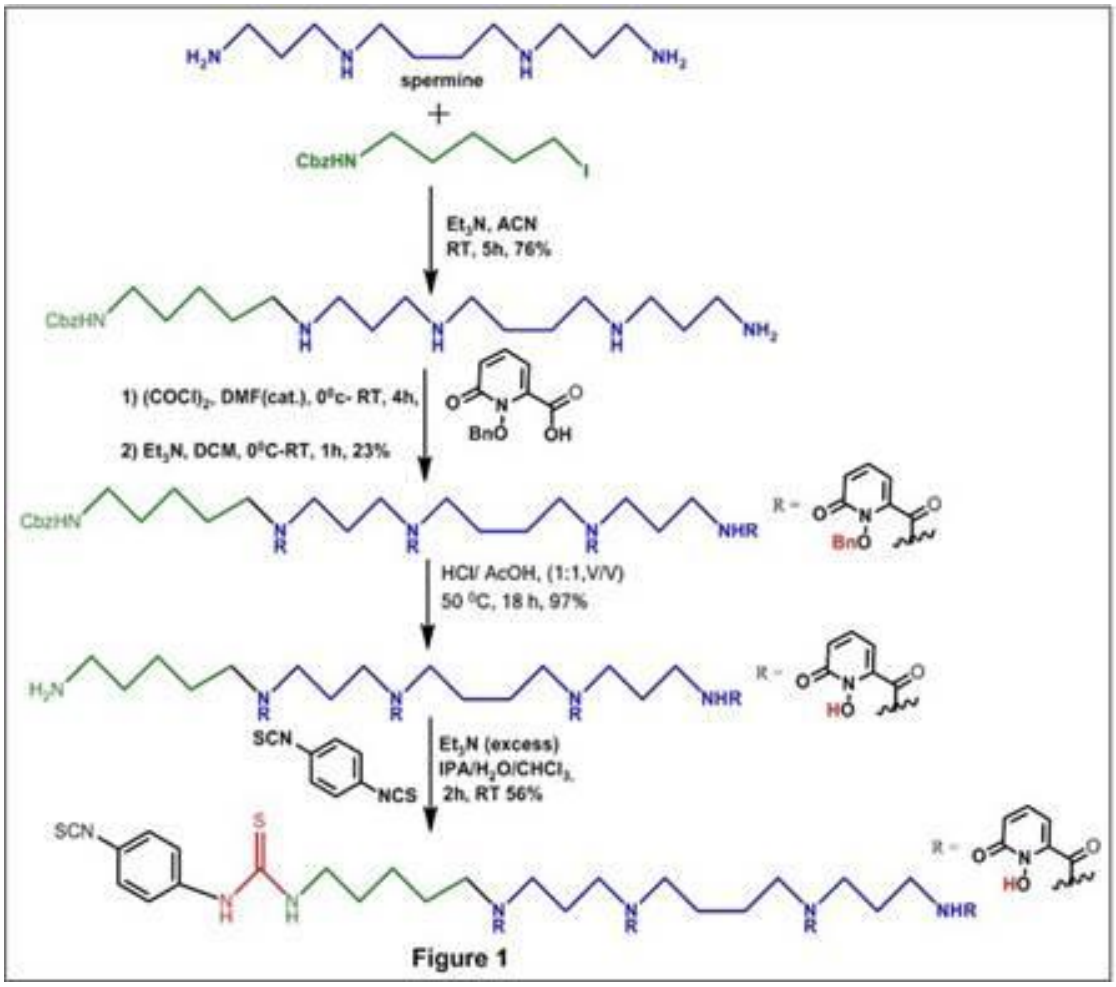

Figure 1

Methods: *Chemistry:* Figure 1 shows the scheme for synthesis of one ligand. Briefly, *N*-protected amino-alkyl iodide was reacted with spermine. The monosubstituted spermine derivative was reacted with HOPO acid chloride to obtain a substituted spermine-HOPO derivative. The amino protecting group from the spermine-HOPO derivative was hydrolyzed by acid, and the amino-alkyl-spermine-HOPO reacted with phenylene-di-isothiocyanate to obtain *p*-SCN-phenyl-alkyl-spermine-HOPO.

Conjugation and radiolabeling: p-SCN-phenyl-C5-spermine-HOPO was conjugated with human or bovine serum albumin and purified, and the

conjugated proteins were radiolabeled with ^{89}Zr-oxalate. After purification on a PD-10 column, the products were tested for *in vitro* stability and biodistribution. *Animal study:* Two groups of healthy athymic nude mice (n=4/group) were intravenously injected with ^{89}Zr-HOPO-BSA or ^{89}Zr-DFO-BSA (12-20 μCi) in phosphate-buffered saline. Mice were scanned every 24 hours up to 48 hours for positron emission tomography. After imaging, all mice were sacrificed; their blood, muscle, bone, heart, lungs, liver, spleen, pancreas, intestines, stomach, and kidneys were isolated and weighed; and their radioactivity was measured using a gamma counter. Radioactivity accumulation was expressed as percent injected dose per gram (%ID/G) and averaged with standard deviation.

Results: We synthesized HOPO analogs in four steps with an overall yield of 10%. The stability of ^{89}Zr-HOPO-albumin in both human and mouse serum and at different pH (5, 6, 7, and 8) remained intact and exhibited better stability than that of ^{89}Zr-DFO-albumin. Preliminary biodistribution of ^{89}Zr-HOPO-protein in normal mice indicated good stability and greater uptake in the liver, spleen, and kidneys.

Conclusion: We achieved radiolabeling of protein with ^{89}Zr using *p*-SCN-phenyl-alkyl-spermine-HOPO with different carbon chain lengths. *In vitro* and *in vivo* stability suggest that ^{89}Zr-labeled protein using HOPO as a chelating agent is more stable than DFO-conjugated products. Further *in vivo* studies with ^{89}Zr-DFO- and ^{89}Zr-HOPO-monoclonal antibodies are in progress for comparison.

References

[1] J. Holand, V. Divilov, N. Bander, et al. *J. Nucl. Med*. **2010**, *51*, 1293-1300.

[2] M. Deri, S. Ponnala, B. Zeglis, et al. *J. Med. Chem*. **2014**, *57*, 4849-4860.

[3] M. Deri, S. Ponnala, P. Kozlowski, et al. *Bioconjugate Chem*. **2015**, *26*, 2579-2591.

Identifying smokers at higher risk for relapse: Validation of a neuroimaging-based classification algorithm

David W. Frank[1], Menton E. Deweese[1], Maher Karam-Hage[1], Jason D. Robinson[1], Damon J. Vidrine[2], Paul M. Cinciripini[1], Francesco Versace[1]

[1]Department of Behavioral Science, The University of Texas MD Anderson Cancer Center, Houston, TX; [2]Oklahoma Tobacco Research Center, University of Oklahoma, Oklahoma City, OK.

Progress in basic neuroscience has improved our understanding of addiction neurobiology, but translating this knowledge into effective relapse-preventing treatments has proven to be difficult.[1] Recently, we reported that smokers with larger event-related potentials (a direct measure of brain activity) to cigarette-related cues compared with pleasant stimuli (C>P) are more likely to have relapses than are smokers with the opposite brain reactivity profile (P>C). We hypothesized that this *neurobiological marker could be used to identify smokers with high vulnerability to relapse.* In this study, we aimed to 1) build a classification algorithm to identify, on a case-by-case basis, smokers characterized by the P>C or C>P event-related potential profiles and 2) validate the clinical relevance of this classification algorithm using an independent data set in which we assessed smoking abstinence during quit attempts by smokers classified as P>C or C>P. To build the classification algorithm, we applied discriminant function analysis to a data set in which we originally observed a significant association between smoking abstinence and neural reactivity to

emotional stimuli. We confirmed the predictive validity of the classification algorithm in an independent data set that included new data from 177 smokers interested in quitting. For each participant, we collected event-related potentials to emotional images before the quit attempts and assessed smoking abstinence 12 months after the quit attempts. Using brain responses, the algorithm classified 111 smokers as P>C and 66 as C>P. A low overall abstinence rate notwithstanding (8.5% of the sample achieved CO-verified 12-month abstinence), individuals classified as P>C were 2.5 times more likely to be abstinent than were smokers classified as C>P (12.0% vs. 4.8%). Although this difference was not statistically significant (p=0.08), these results suggest that neuroimaging techniques can help advance our knowledge of the neurobiological underpinnings of nicotine addiction and improve clinical applications.

Reference

[1] B.J. Everitt. *Eur. J. Neurosci.* **2014**, *40*, 2163-2182.

BASIC RESEARCH

Lipocalin 2 promotes inflammatory breast cancer tumorigenesis and skin invasion

Emilly Schlee Villodre[1,10], Richard Larson[2,10], Xiaoding Hu[1,10], Shane R. Stecklein[2,10], Kristen Gomez[6], Pascal Finetti[8], Savitri Krishnamurthy[5,10], Cristina Ivan[3], Xiaoping Su[4], Naoto T. Ueno[1,10], Steve Van Laere[7], Francois Bertucci[8], Debu Tripathy[1,10], Pablo Vivas-Mejía[9], Wendy A. Woodward[2,10], Bisrat G. Debeb[1,10]

[1]Department of Breast Medical Oncology, The University of Texas MD Anderson Cancer Center, Houston TX; [2]Department of Radiation Oncology, The University of Texas MD Anderson Cancer Center, Houston, TX; [3]Department of Experimental Therapeutics, The University of Texas MD Anderson Cancer Center, Houston, TX; [4]Department of Bioinformatics and Computational Biology, The University of Texas MD Anderson Cancer Center, Houston, TX; [5]Department of Pathology, The University of Texas MD Anderson Cancer Center, Houston, TX; [6]Department of Biological Sciences, The University of Texas at Brownsville, Brownsville, TX; [7]Department of Oncology, University of Antwerp, Antwerpen, Belgium; [8]Department of Medical and Predictive Oncology Aix-Marseille Université, Inserm, CNRS, Institut Paoli-Calmettes, CRCM, Marseille, France; [9]Department of Biochemistry and Cancer Center, University of Puerto Rico, San Juan, PR; [10]Morgan Welch Inflammatory Breast Cancer Clinic and Research Program, The University of Texas MD Anderson Cancer Center, Houston, TX.

Background: Inflammatory breast cancer (IBC) is the most lethal form of primary breast cancer and accounts for a significant percentage of breast cancer deaths in the United States (10%) owing to its aggressive proliferation and metastasis and a lack of effective therapeutic options. Unraveling the underlying mechanisms of growth and metastasis of this aggressive disease could lead to effective therapeutic strategies that improve outcomes in IBC patients. We recently generated *in vitro* and *in vivo* IBC models for brain metastasis studies[1] and observed dramatic upregulation of lipocalin-2 (LCN2), a small, secreted iron-trafficking protein that plays a significant role in immune and inflammatory responses and the promotion of malignant progression. We hypothesized that LCN2 facilitates progression and metastasis of IBC.

Methods: Stable knockdown (KD) of LCN2 in IBC cell lines was achieved with lentiviral vectors. Proteomic and gene expression profiling were performed using a reverse-phase protein array and Affymetrix Clariom D microarray. For *in vivo* studies, control and LCN2-KD IBC cells were transplanted into the cleared mammary fat pads of severe combined immunodeficiency/beige mice. Tumor-skin involvement was assessed visually during primary tumor growth and tumor excision. *LCN2* gene expression levels in clinical samples were analyzed by the IBC Consortium as well as using public data sets. LCN2 serum levels in IBC patients were measured using an enzyme-linked immunosorbent assay and were correlated with clinicopathological variables and outcome data.

Results: *LCN2* gene expression was higher in IBC than in non-IBC patients ($p=0.00036$) independent of the molecular subtype of breast cancer and higher in more aggressive (triple-negative and HER2+) than in hormone receptor-positive subtypes ($p<0.00001$). LCN2 expression in patient tissue was correlated with reduced overall survival ($p<0.00001$) and metastasis-free survival ($p=0.04$) in non-IBC patients. However, LCN2 expression was not associated with overall survival in IBC patient serum samples. LCN2 expression was also significantly higher in IBC cell lines, their culture media, and brain metastasis sublines than in non-IBC cell lines ($p=0.004$). In IBC cell lines, LCN2 KD reduced proliferation, colony formation, migration, and cancer stem cell properties. *In vivo* silencing of LCN2 in SUM149 cells inhibited primary tumor growth ($p=0.001$) and resulted in a well-differentiated tumor histology. Additionally, LCN2 KD in SUM149 cells significantly reduced skin invasion/recurrence (control LCN2 vs. LCN2-KD cells, 88% vs. 25%; $p=0.01$), suggesting that LCN2 is a mediator of tumorigenesis. Analysis of proteomic data demonstrated changes in major signaling pathways, including PI3K-Akt signaling and EGF/EGF receptor signaling pathways. Mechanistically, LCN2 depletion in SUM149 cells abrogated EGF-induced EGF receptor phosphorylation and extracellular signal-regulated kinase activation.

Conclusions: Our findings suggest that LCN2 drives IBC progression and skin invasion/recurrence potentially via the EGF receptor signaling pathway. Future studies will determine the role of LCN2 in metastasis and pinpoint the detailed mechanisms of LCN2-mediated IBC tumorigenesis and recurrence.

Reference

[1] B.G. Debeb, L. Lacerda, S. Anfossi, et al. *J. Natl Cancer Inst*. **2016**, *108*.

CLINICAL/TRANSLATIONAL RESEARCH

Metabolomic profiling improves prediction of minimal residual disease and reveals potential metabolic vulnerabilities in pediatric acute lymphoblastic leukemia

Jeremy Schraw[1], Jacob Junco[2], Austin Brown[2], Michael Scheurer[2], Karen Rabin[2], Philip Lupo[2]

[1]Department of Medicine, Section of Epidemiology and Population Sciences, Baylor College of Medicine, Houston, TX; [2]Department of Pediatrics, Section of Hematology-Oncology, Baylor College of Medicine, Houston, TX.

Background/Objectives: End-induction minimal residual disease (MRD) is the most important predictor of relapse of pediatric acute lymphoblastic leukemia. However, many relapses occur in MRD-negative patients. We hypothesized that global metabolomic profiling of diagnostic bone marrow plasma can improve prediction of MRD and provide insight into the biology of relapse.

Design/Methods: We retrospectively identified 99 patients who received diagnosis and treatment at Texas Children's Hospital from 2007 to 2015, of whom 39 were MRD-positive and 60 were MRD-negative at end-induction, using a cutoff of 0.01%. Diagnostic bone marrow plasma was subjected to metabolomic profiling via ultra-performance liquid chromatography-tandem mass spectrometry. The nonparametric Kruskal-Wallis test was used to compute univariate p values comparing MRD-positive and -negative plasma, and

metabolite set enrichment analysis was used to identify pathways enriched in differentially abundant metabolites with the Kyoto Encyclopedia of Genes and Genomes as the reference. Metabolites with univariate p values up to 0.001 were evaluated in logistic regression models for MRD, and the best predictors were obtained via backward elimination. The performance of models for MRD was assessed using clinical features alone and clinical features plus metabolites via DeLong's test for correlated receiver operating characteristic curves. Also, the *in vitro* cytotoxicity of drugs targeting top-scoring pathways in acute lymphoblastic leukemia cell lines was measured using flow cytometric staining for annexin V/propidium iodide.

Results: Metabolite set enrichment analysis revealed central carbon metabolism to be the pathway most enriched in differentially abundant metabolites (p=4.00E-06). The levels of the constituent metabolites pyruvate, succinate, fumarate, and malate were all significantly increased in MRD-positive patients (p≤0.001). A predictive model for MRD incorporating these metabolites outperformed clinical features alone (area under the curve, 0.86 vs. 0.73; p=0.001). FK866, a nicotinamide phosphoribosyltransferase inhibitor that depletes these metabolites, exhibited significant cytotoxicity in five of six acute lymphoblastic leukemia cell lines (half-maximal inhibitory concentrations, 1-10 nM).

Conclusion: Metabolomic profiling improved prediction of subsequent MRD and identified potentially druggable metabolic alterations. If validated, these

biomarkers may improve risk prediction and our understanding of disease biology.

Poster Presentations

A total of 54 posters were accepted for presentation during the 2018 symposium. The names of the presenting postdocs are shown in boldface.

Please note that only abstracts of presenters who agreed to have their abstracts published are included.

A hybrid agent-based particle and partial differential equations method to analyze vascular adaptation

Marc Garbey[1,2,3], **Stefano Casarin[1,3]**, Scott A. Berceli[4,5]

[1]Center for Computational Surgery, Houston Methodist Research Institute, Houston, TX; [2]Department of Surgery, Houston Methodist Hospital, Houston, TX; [3]LaSIE, UMR CNRS 7356, University of La Rochelle, La Rochelle, France; [4]Department of Surgery, University of Florida, Gainesville, FL; [5]Malcom Randall VAMC, Gainesville, FL.

Introduction: Peripheral arterial occlusive disease is a chronic pathology affecting at least 8-12 million people in the United States that is typically treated with a vein graft bypass or deployment of a stent to restore the physiological circulation. Failure of peripheral endovascular interventions occurs at the intersection of vascular biology, biomechanics, and clinical decision-making. We hypothesize that the majority of endovascular treatment approaches share the same driving mechanisms and that a deep understanding of the adaptation process is pivotal to improving outcomes of the procedure. The postsurgical adaptation of vein graft bypasses offers the perfect example of how the balance between intimal hyperplasia and wall remodeling determines the failure or success of the intervention.

Methods: Presented is a versatile computational model able to capture the feedback loop that describes the interaction between events at the cellular/tissue

level and mechano-environmental conditions. This work is a generalization and improvement of a previous work by our group of investigators in which the graft is approximated as a thick cylinder and an agent-based model is used as a cellular automaton principle on a fixed hexagonal grid to reproduce the leading events of the graft's restenosis.

Results: The new hybrid model facilitates a more realistic simulation of both the biological laws that drive cellular behavior and the active role of the membranes that separate the various layers of a vein. The novel feature is use of an immersed boundary implementation of a highly viscous flow to represent cellular motility and matrix reorganization in response to graft adaptation. Our implementation is modular, which makes us able to choose the right compromise between closeness to the physiological reality and complexity of the model. Finally, quantitative cross-validation with previously developed and validated zero-D models and qualitative validation with histological data from a rabbit model of intimal hyperplasia has been conducted, with satisfactory results.

Discussion: Our model offers a new modular implementation that combines the best features of an agent-based model, continuum mechanics, and particle-tracking methods to cope with the multiscale nature of the adaptation phenomenon. This hybrid method enables us to quickly test various hypotheses, with particular attention to cellular motility, a process that we demonstrated should be driven by mechanical homeostasis to maintain the right balance

between cells and the extracellular matrix to reproduce a distribution similar to histological experimental data from vein grafts.

Conclusion: A detailed description of the complex network that regulates restenosis phenomena offers great potential to control the disease, driving therapy toward a better outcome.

Nanofluidic drug-eluting seed for sustained intratumoral immunotherapy for cancer treatment

Corrine Ying Xuan Chua[1], Antonio Susnjar[1], Jeremy Ho[1], Jessica Rhudy[1], Priya Jain[1], Marco Folci[1,2], Andrea Ballerini[1,3], April Gilbert[1], Shailbala Singh[4], Giacomo Bruno[1,5], Cassian Yee[4], Brian E. Butler[1], Alessandro Grattoni[1]

[1]Department of Nanomedicine, Houston Methodist Research Institute, Houston, TX; [2]Department of Allergy and Clinical Immunology, Istituto Auxologico Italiano, University of Milan, Milan, Italy; [3]Department of Medical Biotechnology and Translational Medicine, University of Milan, Milan, Italy; [4]Department of Melanoma Medical Oncology, The University of MD Anderson Cancer Center, Houston, TX; [5]Politecnico di Torino, Turin, Italy.

Although the clinical breakthrough of treatment with immune checkpoint inhibitors such as nivolumab and ipilimumab in certain cancers has fueled optimism about immunotherapy, its efficacy is limited to a small subset of patients. In addition to insufficient antitumor immune response, systemic administration causes adverse side effects, with up to 91% of treated patients experiencing clinically significant immune-related adverse events. Intratumoral immunotherapy delivery has demonstrated antitumor efficacy in preclinical and clinical studies with minimal systemic toxicity. However, despite encouraging results, the feasibility of intratumoral injection is restricted to accessible solid tumors, whereas inaccessible tumors require technically challenging image-guided injections. To fulfill the unmet need for sustained local drug delivery and avoid repeated

intratumoral injections, we developed the nanofluidic drug-eluting seed (NDES), a device the size of a grain of rice, for intratumoral drug delivery. The NDES is inserted intratumorally using a minimally invasive trocar-based method similar to brachytherapy seed insertion and offers the clinical benefit of drug elution. Drug release from the NDES is driven by a difference in concentration, allowing for sustained intratumoral immunotherapy delivery without the need for injections, actuation, or clinician intervention. In this study, we used the NDES to deliver immunotherapy intratumorally in the 4 T1 orthotopic murine mammary carcinoma model, which recapitulates triple-negative breast cancer. We demonstrated that NDES-mediated intratumoral release of the agonist monoclonal antibodies OX40 and CD40 resulted in potentiation of local and systemic antitumor immune response and inhibition of tumor growth, unlike the control treatment. Furthermore, mice given NDES-CD40 had minimal systemic drug exposure and liver damage in contrast with systemically treated mice. Because CD40-based monotherapy was insufficient to eliminate tumor burden, we speculated that maximal therapeutic synergy could be achieved using combination treatment with radiation to induce immunogenic cell death. In line with this, in combination with localized irradiation, NDES-CD40 was more effective at reducing tumor burden than was monotherapy. Overall, we found that the NDES is an effective platform for sustained intratumoral immunotherapy delivery with potential for clinical translation given that the NDES is applicable to a broad spectrum of drugs and solid tumors.

An Exploratory factor analysis of patient-centered cancer care measures to support improved assessment of patients' experiences

Kerri-Anne Parkes[1], Bryan Fellman[2], Kelly Brassil[1]

[1]Department of Nursing, The University of Texas MD Anderson Cancer Center, Houston, TX; [2]Department of Biostatistics, The University of Texas MD Anderson Cancer Center, Houston, TX.

Background: Cross-cutting quality measures developed with strong psychometric properties and patient input are critical to assessing and achieving high-quality patient-centered cancer care.

Objective: In the present study, patient-centered cancer care dimensions were examined using exploratory factor analysis, and their relationships with demographic characteristics and cancer site were assessed.

Methods: Exploratory factor analysis was performed using the modified Patients and the Cancer Care Experience Survey, a patient-reported measure of perceived importance of social, emotional, physical, and informational aspects of cancer care administered to adult patients at a National Cancer Institute-designated comprehensive cancer center. Bivariate analyses were performed using the Wilcoxon rank-sum test.

Results: The exploratory factor analysis revealed a five-factor model: 1) quality of life, 2) provider social support, 3) psychosocial needs, 4) nonprovider social support, and 5) health information and decision-making support. We found statistically significant associations between these factors and patients' demographic characteristics and cancer sites. Female participants (p=0.036) and those younger than 60 years (p=0.036) were more concerned about quality of life. Participants with prostate cancer were more concerned about social support from providers (p=0.035) and psychosocial needs (p=0.002). Lung cancer patients were less concerned about psychosocial needs (p=0.029).

Conclusions: All of the dimensions of existing patient-centered care models were supported by the identified model. One exception, care coordination, was not significant, perhaps due to overlap with another factor or the small sample size. Increased understanding of patient-centered cancer care and its associations with patient characteristics can support practice changes to improve patients' cancer care experiences.

Automated image quality evaluation of structural brain magnetic resonance images using deep convolution neural networks

Sheeba J. Sujit[1], Refaat E. Gabr[1], Ivan Coronado[1], Melvin Robinson[2], Sushmita Datta[1], Ponnada A. Narayana[1]

[1]Department of Diagnostic and Interventional Imaging, The University of Texas Health Science Center at Houston, Houston, TX; [2]Department of Electrical Engineering, The University of Texas at Tyler, Tyler, TX.

Automated evaluation of image quality is essential to assuring accurate diagnosis and patient management. This is particularly important for multicenter studies, typically employed in clinical trials, in which data are acquired using different machines with different protocols. Visual quality assessment of magnetic resonance imaging (MRI) is subjective and impractical for large data sets. Data-intensive deep learning methods such as convolutional neural networks (CNNs) are promising tools for processing large-scale imaging data sets for automated quality assessment. In this study, we focused on quality evaluation of the Autism Brain Imaging Data Exchange structural brain MRI data set acquired from 17 sites on more than 1000 subjects using CNNs. The multilayer deep learning architecture consisted of an input layer, four convolution layers, two fully connected layers, and an output layer. We selected 378 image volumes to balance between the acceptable and unacceptable based on expert evaluation. Sixty percent of the data were used for training, 15% were used for validation, and 25% were used for testing. The results of the automated approach were

compared with evaluation by a radiologist. Performance of the CNN was assessed using a confusion matrix from which the sensitivity, specificity, and accuracy were calculated. The concordance in the image quality label between the expert and CNN was 86% (sensitivity, 81%; specificity, 92%). This study demonstrated that the proposed algorithm can be used to evaluate the quality of brain MRI with greater classification accuracy than previous state-of-the-art classical machine learning algorithms. We did all processing using the *Maverick 2* cluster at the Texas Advanced Computing Center in Austin, TX. We used NVIDIA Tesla GTX graphical processing unit cards and carried out implementation in the Python computing language using the Keras library and TensorFlow.

Inhibition of autophagy kinase ULK1 combined with chemotherapy results in modulation of reactive oxygen species and DNA damage response to induce synergistic cell death in acute myeloid leukemia

Seemana Bhattacharya, Sujan Piya, Teresa McQueen, Marina Konopleva, Michael Andreeff, Gautam Borthakur

Department of Leukemia, The University of Texas MD Anderson Cancer Center, Houston, TX.

Introduction: Cytarabine (Ara-C)-based chemotherapy has been the backbone of acute myeloid leukemia (AML) treatment, but relapses are common in adults. Targeted therapies are approved for only a few specific mutations and yield limited responses. Several chemotherapeutic agents used in AML chemotherapy induce cytoprotective autophagy, conferring drug resistance.[1] Autophagy protects quiescent hematopoietic stem cells from metabolic stress by maintaining low intracellular reactive oxygen species (ROS) levels.[2] Impaired autophagy is associated with increased oxidative metabolism, and ROS production causes loss of quiescence due to oxidative stress.[3] Leukemic stem cells are more dependent on oxidative metabolism and, hence, more sensitive to oxidative stress.[4]

Our previous work demonstrated that autophagy inhibition (genetic knockdown of Atg7) enhances AML sensitivity to standard therapies (Ara-C and idarubicin).[5]

Because ULK1 is an apical kinase in the autophagy pathway, we hypothesized that targeting ULK1 can inhibit autophagy and alter intracellular ROS in AML cells. This would help overcome chemoresistance by modulating ROS. We also elucidated the mechanistic details.

Methods: ULK1 expression was genetically altered in OCI-AML3 human AML cells by shRNA-knockdown or CRISPR/Cas9 knockout. In addition, AML cells and patient samples were treated with Ara-C and the ULK1 inhibitor SBI-0206965.[6] The combination index for drug synergy was calculated based on the Chou-Talalay method.[7] Autophagy was detected using LC3 quantification (Western blotting and flow cytometry) and acridine orange and monodansylcadaverine assays. Other assays used were ROS, mass cytometry (cytometry by time of flight), reverse-phase protein array, glutathione, Western blotting, and real-time PCR.

Results: Ara-C induced autophagy (twofold to fourfold in all assays). ULK1 knockdown/knockout enhanced Ara-C–mediated cytotoxicity by 25% ± 3% and 47% ± 5%, respectively ($p<0.01$). Similarly, concomitant treatment with the ULK1 inhibitor SBI-0206965 enhanced Ara-C–induced death of OCI-AML3 (from 44% to 60%; $p=0.23$) and MOLM13 (from 33% to 85%; $p=0.0003$) cells over that by ara-C alone. The combination was also effective in eliminating bulk and CD34+ stem/progenitor populations among primary AML cells (combination index: bulk, 0.68; CD34+, 0.69; $p<0.05$).

SBI-0206965 alone induced ROS in AML cells (62% ± 13%; p=0.013). This was associated with ATM activation and DNA damage (PARP and caspase 3 cleavage, H2AX phosphorylation). The ROS quencher *N*-acetylcysteine could partially mitigate the DNA damage, confirming the role of ROS in that damage (shown via Western blotting). Ara-C increased ROS levels (62% ± 3%; p=0.004), and the combination with SBI-0206965 further enhanced ROS generation (115% ± 9%; p=0.01). Again, *N*-acetylcysteine reduced ROS levels to 42% (p=0.011). Thus, the combination generated excess ROS, which accounts for increased DNA damage.

Mechanistically, an increased ROS level upon ULK1 inhibition was associated with intracellular glutathione. Glutathione is regulated by the cysteine-glutathione antiporter system (xCT/CD44). ULK1 inhibition by SBI-0206965 downregulated transcripts of CD44 and its variant (v8-10) by 86% and 81%, respectively (p=0.001). The xCT and CD44 proteins were also downregulated. When we injected control and ULK1-knockout cells into NSG mice, we observed a marked delay in leukemia engraftment in the ULK1-knockout group. Further studies are ongoing.

Conclusions: Autophagy prevents maximal apoptosis induced by chemotherapy in AML cells. Our study demonstrated single-agent activity of the ULK1 inhibitor SBI-0206965 and enhanced efficacy of chemotherapy combined with ULK1

inhibition. This combination potentiates chemotherapy-induced DNA damage by reversing drug-induced autophagy and modulating intracellular ROS through xCT/CD44.

References

1. J. Zhang. W. Lei, X. Chen, et al. *Mol Clin Oncol*. **2018**, 8 (3),391-399.
2. M. Mortensen, E.J. Soilleux, G. Djordjevic, et al. *J Exp Med*. **2011**, 208, 455-67.
3. T.T. Ho, M.R. Warr, E.R. Adelman, et al. *Nature*. **2017**.543 (7644), 205-210.
4. J. Cheong, Y. Kim, J.I. Eom, et al. *Mol Med Rep*. **2016**,13 (4), 3433-3440.
5. S, Piya, S.M. Kornblau, V.R. Ruvolo, et al. *Blood*. **2016**,128 (9), 1260-1269.
6. D.F. Egan, M.G.H. Chun, M. Vamos, et al. *Mol Cell*. **2015**, 59(2), 285-297.
7. T. Chou *Can Res*. **2010**, 70(2), 440-446.

TP73 isoforms (TAp73 and ΔNp73) are overexpressed in acute myeloid leukemias and potential therapeutic targets to enhance anti-leukemia activities of Bcl-2 and MDM2 inhibitors

Yuki Nishida, Jo Ishizawa, Vivian R. Ruvolo, Michael Andreeff

Department of Leukemia, The University of Texas MD Anderson Cancer Center, Houston, TX.

Background: *TP73* is one of the *TP53* family transcription factors and generates two isoforms, transactivation of p73 (TAp73) and N-terminally truncated p73 (ΔNp73). TAp73 shares a homologous N-terminal activation domain with p53 and has proapoptotic function similar to that of p53. ΔNp73 lacks an activation domain and has activities distinct from those of TAp73. ΔNp73 has a dominant-negative effect on the DNA binding of TAp73 and, more importantly, p53, as the DNA-binding domain is homologous with that of TAp73 and highly similar to that of p53. Authors have reported *TP73* to be expressed in acute myeloid leukemia (AML) cells but not acute promyelocytic leukemia cells. However, the association of *TP73* isoforms with clinical and genetic characteristics of and regulation of the isoforms in AML cases have yet to be explored.

Results: We determined copy numbers of *ΔNp73* and *TAp73* mRNA levels in 78 AML samples, including 31 *de novo* AML samples, using droplet digital PCR (ddPCR), and investigated their clinical and biological relevance. We detected *ΔNp73* and *TAp73* expression in 93.6% and 98.7% of AML samples,

respectively, at various levels (mean [± standard error of the mean], 10.6 ± 5.0 and 106.6 ± 33.7 copies/μL for *ΔNp73* and *TAp73*, respectively). *ΔNp73* and *TAp73* mRNA levels were highly correlated (R^2 = 0.72; p<0.0001). Normal peripheral blood mononuclear cells and CD34+ hematopoietic cells had little or no *ΔNp73* or *TAp73* expression (0.09 ± 0.09 and 0.42 ± 0.35 copies/μL, respectively), demonstrating that expression of *ΔNp73* and *TAp73* is 100-fold to 1000-fold higher in AML cells than in normal hematopoietic cells. Disease status (*de novo* or relapsed/refractory) and cytogenetic abnormalities did not correlate with *ΔNp73* or *TAp73* levels. However, AML cells with *IDH1/2* mutations had 8.5-fold lower *ΔNp73* expression than did those with wild-type *IDH1/2* (1.8 ± 0.8 vs. 15.4 ± 7.7 copies/μL; p=0.0069), with a similar trend for *TAp73* (49.0 ± 20.3 vs. 138.6 ± 51.4 copies/μL; p=0.056). To further explore regulation of *TP73* isoforms, we used the MDM2 inhibitor Nutlin-3a to induce expression of p53, which is a transcriptional inducer of *ΔNp73*. Nutlin-3a increased p73 protein levels, and knockdown of both TAp73 and ΔNp73 in AML cells enhanced apoptosis induction (specific annexin V induction, 21.9% ± 1.3% vs. 61.3% ± 5.2%; p=0.0084 in OCI-AML3 cells with vector control vs. Shp73, respectively), possibly due to silencing of *ΔNp73*. AML cells with *IDH1/2* mutations are more dependent on Bcl-2 than are those without them.[1] Of note, (R)-2HG, the oncometabolite of mutant *IDH1/2*, reduced both *TAp73* and *ΔNp73* levels in AML cells and increased susceptibility to the Bcl-2 inhibitor ABT-199.

Conclusion: Absolute quantitation of *TP73* isoforms using ddPCR revealed higher expression in AML cells than in normal hematopoietic cells. Repressed expression of *TP73* isoforms in AML cells with *IDH1/2* mutations or by the oncometabolite (R)-2HG suggests that epigenetic modifications via (R)-2HG can regulate *TP73* transcription and enhance the antileukemia effect by Bcl-2 inhibition. Finally, downregulation of *TP73* isoforms enhances the efficacy of MDM2 inhibitor against AML, suggesting a therapeutic strategy to enhance MDM2 inhibitor-mediated p53 activation.

Reference

[1] S.M. Chan, D. Thomas, M.R. Corces-Zimmerman, et al. *Nat. Med*. **2015**, *21*, 178-184.

The expression of MIF-regulated inflammatory markers in stage IV melanoma: Risk of CNS metastasis and survival

Dai Ogata[1], Sun-Hee Kim[1], Jason Roszik[1,2], Roland L. Bassett Jr.[3], Elizabeth A. Grimm[1], Suhendan Ekmekcioglu[1]

[1]Department of Melanoma Medical Oncology, The University of Texas MD Anderson Cancer Center, Houston, TX; [2]Department of Genomic Medicine, The University of Texas MD Anderson Cancer Center, Houston, TX; [3]Department of Biostatistics, The University of Texas MD Anderson Cancer Center, Houston, TX.

Purpose: Chronic inflammation is known to be associated with melanoma progression. We sought to determine which inflammatory marker's expression in stage IV melanomas is associated with outcome and whether increased expression of inflammatory markers in systemic non-central nervous system (CNS) melanoma metastasis is associated with increased risk of CNS metastasis and is a negative prognostic factor for overall survival.

Methods: We retrospectively identified 315 patients with stage IV melanoma. Using a tissue microarray of systemic non-CNS metastasis specimens from these patients, we performed immunohistochemical analysis to measure the cellular expression of CD74, macrophage migration inhibitory factor, inducible nitric oxide synthase, nitrotyrosine, cyclooxygenase-2, and microsomal prostaglandin E synthase-1. We analyzed the association of these inflammatory

markers with median survival and time to first CNS metastasis using a Kaplan-Meier survival curve.

Results: Expression of CD74 impacted overall survival of stage IV melanoma (p=0.0196). The combination of CD74 positivity and macrophage migration inhibitory factor negativity provided an overall survival advantage in the patients (p=0.0264). Expression of CD74 tended to be predictive of development of or time to CNS metastasis, and expression of nitrotyrosine impacted development of or time to CNS metastasis.

Conclusions: Our data validated CD74 as a useful prognostic tumor cell protein marker associated with favorable overall survival in stage IV melanoma patients. Nitrotyrosine expression was associated with increased time to CNS metastasis.

BET bromodomain protein 4 as a novel therapeutic target in dilated cardiomyopathy in laminopathy

Gaëlle Auguste[1], Priyatansh Gurha[1], Scot Matkovich[2], Raffaella Lombardi[1], Ali J. Marian[1]

[1]*Center for Cardiovascular Genetics, Institute of Molecular Medicine, The University of Texas Health Science Center at Houston, Houston, TX;* [2]*Center for Pharmacogenomics, Department of Internal Medicine, Washington University School of Medicine, St. Louis, MO.*

Lamin A/C (LMNA) is a major component of the inner nuclear membrane and is involved in regulation of gene expression. Mutations of the *LMNA* gene cause a heterogeneous group of diseases that are collectively referred to as laminopathies. Cardiac involvement is one of the most prominent features of laminopathies, presenting with dilated cardiomyopathy (DCM), conduction defects, and sudden death. Molecular mechanisms involved in the pathogenesis of cardiac phenotypes in laminopathies are not well known. To gain insight into molecular pathogenesis of DCM caused by LMNA deficiency, the *Lmna* gene was deleted exclusively in cardiac myocytes (*Myh6-Cre:Lmna*^{Flox}). Homozygous (*Myh6-Cre:Lmna*$^{F/F}$) mice were born at the expected Mendelian ratio and had normal cardiac function and histology at 2 weeks of age. However, the mice had progressive cardiac dilatation and dysfunction, interstitial fibrosis, and increased apoptosis and died by 4 weeks of age. Heterozygous mice (*Myh6-Cre:Lmna*$^{W/F}$) have a milder phenotype that starts at 6 months of age. To identify transcriptomic

changes that precede cardiac dilatation and dysfunction, cardiac myocytes were isolated from 2-week-old wild-type and *Myh6-Cre:Lmna*$^{F/F}$ mice and analyzed using RNA sequencing. A total of 1420 genes were differentially expressed in wild-type and *Myh6-Cre:Lmna*$^{F/F}$ myocytes. Pathway analysis of differentially expressed genes demonstrated enrichment of inflammatory, epithelial-to-mesenchymal transition, and cell death pathways, whereas mitochondrial oxidative function, adipogenesis, and fatty acid metabolism pathways were depressed in *Myh6-Cre:Lmna*$^{F/F}$ mice. Ingenuity Pathway Analysis identified BET bromodomain protein 4 (BRD4) among the top five upstream regulators of the differentially expressed genes. Consistently, treatment with the BET bromodomain inhibitor JQ1 improved survival and cardiac function in the *Myh6-Cre:Lmna*$^{F/F}$ mice over that in untreated and vehicle-treated *Myh6-Cre:Lmna*$^{F/F}$ mice. Effects on the myocardial phenotypes (e.g., apoptosis, fibrosis) are being analyzed.

In conclusion, LMNA deficiency results in dysregulation of a large number genes, including BRD4 target genes that precede the onset of cardiac dysfunction and fibrosis. The findings point to the prominent role of BRD4 in development of cardiac dysfunction in cases of myocyte-specific LMNA deficiency and identify this protein as a therapeutic target DCM caused by LMNA deficiency.

Emerging role for membrane therapy in shaping aberrant Wnt signaling

Alfredo Erazo-Oliveras, Natividad R. Fuentes, Michael L. Salinas, Kerstin K. Landrock, Robert S. Chapkin

Program in Integrative Nutrition & Complex Diseases and Center for Translational Environmental Health Research, Texas A&M University, College Station, TX.

Wnt signaling is the major driving force behind homeostatic self-renewal of the intestinal crypt. Dysregulation of Wnt signaling has been linked with cancer in multiple types of tissue. For example, about 90% of colorectal cancer (CRC) cases are associated with defects in this pathway. In the vast majority (>80%) of sporadic CRC cases, sequencing evidence indicates the presence of mutations of adenomatous polyposis coli (APC). This gatekeeping gene is a key regulator of Wnt signaling. Loss of *Apc* function causes aberrant stabilization of β-catenin, a crucial step in CRC initiation. Notably, attempts to target this pathway using drugs still face multiple hurdles due to poor tumor-cell targeting and kill specificity, negative side effects associated with required long-term treatment, and poorly understood mechanisms of action. Consequently, additional mechanistic insight into the Wnt signaling pathway is urgently needed to develop toxicologically innocuous therapeutic approaches. With respect to Wnt signaling transduction, two key plasma membrane receptors, LRP5/6 and Frizzled (Fz), require lipid raft localization and nanoclustering with cytosolic Dvl and Axin for

efficient signaling. Various effectors (e.g., nystatin, Dkk1) that disrupt lipid raft dynamics alter LRP5/6 and Fz clustering and downstream signaling, leading to a reduction in β-catenin stabilization. Thus, we examined the effect of oncogenic APC (oAPC) on key colonocyte plasma membrane lipid-lipid, lipid-protein, and protein-protein interactions of Wnt-associated effectors in a conditionally mutated mouse model of CRC and oAPC-expressing cell lines. We showed for the first time that oAPC significantly increased the levels of free cholesterol in the plasma membrane, a major component of lipid rafts known to selectively activate canonical Wnt signaling. Moreover, oAPC significantly increased lipid-lipid interactions, for example, plasma membrane rigidity and lipid raft stability. We subsequently examined the effect of oAPC on the spatiotemporal dynamics (protein-protein clustering) of Wnt signaling receptors/effectors in a CRC cell line model expressing oAPC. oAPC significantly increased LRP5/6 and Fz homoclustering and LRP5/6-Fz heteroclustering, resulting in enhancement of Wnt signaling. Of note, the dysregulation of plasma membrane physical/chemical properties described above was exacerbated when a constitutively active form of β-catenin was expressed in oAPC cell lines. Collectively, these findings demonstrate that oAPC can directly perturb cholesterol homeostasis in colonocytes, thereby altering lipid raft stability, plasma membrane LRP5/6 and Fz clustering, and downstream Wnt signaling. Thus, loss of plasma membrane homeostasis is a key step in CRC initiation, demonstrating the importance of developing membrane-targeted therapies.

Long chain n-3 fatty acids attenuate oncogenic KRas-driven proliferation by altering plasma membrane nanoscale proteolipid composition

Natividad R. Fuentes[1], Mohamed Mlih[2], Rola Barhoumi[3], Yang-Yi Fan[1], Paul Hardin[4], Trevor J. Steele[5], Spencer Behmer[5], Ian A. Prior[6], Jason Karpac[2], Robert S. Chapkin[1,7]

[1]Program in Integrative Nutrition & Complex Diseases, Texas A&M University, College Station, TX; [2]Department of Molecular and Cellular Medicine, College of Medicine, Texas A&M Health Sciences Center, College Station, TX; [3]Department of Veterinary Integrative Biosciences, Texas A&M University, College Station, TX; [4]Department of Biology, Texas A&M University, College Station, TX; [5]Department of Entomology, Texas A&M University, College Station, TX; [6]Division of Cellular and Molecular Physiology, University of Liverpool, Liverpool, UK; [7]Center for Translational Environmental Health Research, Texas A&M University, College Station, TX.

Ras signaling originates from transient nanoscale compartmentalized regions of the plasma membrane composed of specific proteins and lipids. The highly specific lipid composition of these nanodomains, termed nanoclusters, facilitates effector recruitment and therefore influences signal transduction. This suggests that Ras nanocluster proteolipid composition represents a novel target for future chemoprevention interventions. Evidence demonstrates that consumption of fish oil containing long-chain n-3 polyunsaturated fatty acids such as

eicosapentaenoic acid ($20:5^{\Delta 5,8,11,14,17}$) and docosahexaenoic acid ($22:6^{\Delta 4,7,10,13,16,19}$) may reduce colon cancer risk in humans, yet the mechanism underlying this effect is unknown. As described herein, we demonstrated that dietary n-3 polyunsaturated fatty acids reduce the lateral segregation of cholesterol-dependent and -independent nanoclusters, suppressing phosphatidic acid-dependent oncogenic KRas effector interactions, via their physical incorporation into plasma membrane phospholipids. This results in attenuation of oncogenic Ras-driven colonic hyperproliferation in both *Drosophila* and murine models. These findings demonstrate the unique properties of dietary n-3 polyunsaturated fatty acids in the shaping of Ras nanoscale proteolipid complexes and support the emerging role of plasma membrane-targeted therapies.

FAT1-REST exhibit a context-dependent relationship in glioblastoma

Khushboo Irshad[1], Yungang Lu[1], Joy Gumin[2], Anantha Marisetty[2], Nelson Iheonunekwu[1], Dimpy Koul[3], Yiling Lu[4], Sadhan Majumder[1]

[1]Department of Genetics, The University of Texas MD Anderson Cancer Center, Houston, TX; [2]Department of Neurosurgery, The University of Texas MD Anderson Cancer Center, Houston, TX; [3]Department of Neuro-Oncology, The University of Texas MD Anderson Cancer Center, Houston, TX; [4]Department of Systems Biology, The University of Texas MD Anderson Cancer Center, Houston, TX.

Background: The role of the protocadherin gene *FAT1* in glioma tumorigenesis is contradictory. *FAT1* modulates stemness genes, including *REST*, *SOX2*, *OCT4*, and *NESTIN*, in the glioblastoma cell lines U87MG and A172 under hypoxic conditions. Whereas hypoxia increases the expression of these stemness markers in U87MG and A172 cells, *FAT1* knockdown results in their downregulation under the same conditions. Hence, we investigated the relationship of *FAT1* with *REST* in a new cell model, patient-derived glioblastoma stem cells (GSCs), which is close to *in vivo* tumors.

Methods: High-REST GSC lines (HR-GSC1 and HR-GSC2) had been derived and established from glioblastoma patients in our laboratory. They were maintained under *in vitro* stemness conditions using Dulbecco's modified Eagle's

medium-F12 medium and epidermal growth factor and B27 supplements. Transient small interfering RNA-mediated *FAT1* knockdown was performed in GSCs exposed to normoxia (20% O_2) and severe hypoxia (0.2% O_2). Quantitative polymerase chain reaction was performed to analyze the expression of *FAT1*, *REST*, and other stemness marker genes in FAT1 small interfering RNA-exposed cells relative to that in control small interfering RNA-exposed cells under both normoxia and hypoxia.

Results: *REST* mRNA expression increased upon exposure to hypoxia in both HR-GSC1 and HR-GSC2. On one hand, in HR-GSC1, *FAT1* knockdown led to decreased *REST* mRNA levels under normoxia as well as hypoxia. This was accompanied by decreases in *SOX2* and *OCT4* mRNA levels. On the other hand, in HR-GSC2, *REST* mRNA levels increased after *FAT1* knockdown under both normoxia and hypoxia. *SOX2* and *OCT4* levels in HR-GSC2 also increased after *FAT1* knockdown under normoxia and hypoxia.

Conclusions: We observed differential modulation of *REST* and other stemness genes by *FAT1* in GSCs as compared with that in the glioblastoma cell lines U87MG and A172. Whereas HR-GSC1 is a cell model similar to U87MG and A172, HR-GSC2 exhibits divergent behavior upon *FAT1* knockdown. Our results support the context-dependent behavior of *FAT1* in glioma and imply that *FAT1*-mediated stemness modulation depends on intervening molecular mechanisms operating in the different cell types. Such patient-to-patient genetic variation

reflects implications in determining personalized therapeutic approaches and should be considered for further study.

Targeted hypoxia reduction restores T cell infiltration and sensitivity to immunotherapy in prostate cancer

Priyamvada Jayaprakash[1], Midan Ai[1,] Arthur Liu[1], Pratha Budhani[1], Todd Bartkowiak[1,2], Jie Sheng[1], Casey Ager[1,2], Courtney Nicholas[1], Ashvin Jaiswal[1,2], Yanqiu Sun[1], Krishna Shah[2], Sadhana Balasubramanyam[1], Nan Li[3], Guocan Wang[4], Jing Ning[3], Anna Zal[1], Tomasz Zal[1,2], Michael A. Curran[2]

[1]Department of Immunology, The University of Texas MD Anderson Cancer Center, Houston, TX; [2]MD Anderson Cancer Center UTHealth Graduate School of Biomedical Sciences, Houston TX; [3]Department of Biostatistics, The University of Texas MD Anderson Cancer Center, Houston, TX; [4]Department of Cancer Biology, The University of Texas MD Anderson Cancer Center, Houston, TX.

T-cell checkpoint blockade with anti-cytotoxic T-lymphocyte-associated protein 4 (CTLA-4) and anti-programmed cell death protein 1(PD-1) therapy is effective against “hot” tumors like melanoma with pre-existing immune infiltrates. However, “cold” tumors like prostate and pancreatic cancers respond poorly. We found that hypoxic zones are prevalent across preclinical prostate cancers and resist T-cell infiltration even in the context of CTLA-4 and PD-1 blockade. Hypoxia fosters metabolic alterations, resulting in extracellular acidification of the microenvironment, depletion of essential amino acids like arginine and tryptophan, accumulation of extracellular adenosine, dense expression of inhibitory ligands like PD-L1 and recruitment and polarization of immature myeloid cells into immunosuppressive myeloid-derived suppressor cells and

tumor-associated macrophages, all of which dampen T-cell responses. For prostate cancer, increased hypoxia has been strongly correlated with more aggressive disease. We used the hypoxia-activated prodrug TH-302 to disrupt tumor hypoxia and showed that it cooperated with checkpoint blockade in curing 80% of mice of TRAMP-C2 prostate tumors. This combination therapy increased T-cell infiltration into previously hypoxic areas concomitant with reduced immunosuppressive myeloid cell infiltration and suppressive function. Tumors from mice receiving TH-302 and checkpoint blockade exhibited persistent defects in their ability to replenish the myeloid stroma. In addition, tumor-infiltrating T cells from TH-302– and checkpoint blockade-treated mice had greater effector cytokine production and mitochondrial biomass than did their untreated counterparts. Spontaneous prostate tumors in TRAMP transgenic mice, which are completely resistant to checkpoint blockade, exhibited minimal adenocarcinoma burden at 36 weeks of age and no evidence of neuroendocrine tumors in response to the combination therapy. Survival of *Pb-Cre4* and *Pten*$^{pc-/-}$*Smad4*$^{pc-/-}$ mice with highly aggressive prostate adenocarcinoma was also significantly extended by the combination of TH-302 and checkpoint blockade. This combination of hypoxia disruption and T-cell checkpoint blockade may render some of the most therapeutically resistant cancers sensitive to immunotherapy.

HDAC6 inhibition prevents cisplatin-induced peripheral neuropathy in a T cell-dependent manner

Jiacheng Ma, Ronnie T. Trinh, Iteeben D. Mahant, Cobi J. Heijnen, Annemieke Kavelaars

Department of Symptom Research, The University of Texas MD Anderson Cancer Center, Houston, TX.

Background: Chemotherapy-induced peripheral neuropathy (CIPN) is a serious health concern for cancer patients receiving chemotherapy, affecting more than 60% of this population. Currently, U.S. Food and Drug Administration-approved drugs to effectively manage CIPN are lacking, emphasizing the urgent need to identify novel agents to prevent CIPN. Histone deacetylase 6 (HDAC6) is a cytosolic deacetylase whose substrates include a-tubulin and Hsp90. We have shown that inhibition of HDAC6 reverses established CIPN in a mouse model through resolution of chemotherapy-induced mitochondrial dysfunction and axonal transport deficits. Currently, the HDAC6 inhibitor ACY-1215 is used in clinical trials as add-on therapy for cancer. Therefore, we sought to determine if adding this HDAC6 inhibitor to chemotherapy prevents CIPN.

Goals: To investigate whether administration of the HDAC6 inhibitor ACY-1215 during cisplatin-based treatment prevents CIPN and, if so, to understand its underlying mechanism.

Methods: CIPN was induced by two cycles of five daily intraperitoneal cisplatin injections. ACY-1215 was given via oral gavage 1 hour prior to each cisplatin injection. Mechanical allodynia in wild-type, T-cell-deficient Rag2-knockout ($Rag2^{-/-}$) and HDAC6-knockout ($HDAC6^{-/-}$) mice was measured using the von Frey test. Mitochondrial bioenergetics were measured using an XF24 Flux Analyzer. For adoptive T-cell transfer, T cells were isolated from the spleens of wild-type and $HDAC6^{-/-}$ mice and injected intravenously into $Rag2^{-/-}$ mice 1 week prior to treatment.

Results: Our data demonstrated that coadministration of ACY-1215 prevents cisplatin-induced mechanical allodynia and neuronal mitochondrial dysfunction. $HDAC6^{-/-}$ mice did not experience cisplatin-induced mechanical allodynia or mitochondrial dysfunction, indicating target specificity of the inhibitor. Intriguingly, we found that the protective effects of the HDAC6 inhibitor did not occur in $Rag2^{-/-}$ mice without mature T and B lymphocytes. Reconstitution of $Rag2^{-/-}$ mice with $CD3^{+}$ T cells restored the effect of the inhibitor, suggesting that HDAC6 inhibition prevents CIPN in a T-cell-dependent manner. To determine whether HDAC6 inhibition in T cells is sufficient to protect against CIPN, we reconstituted $Rag2^{-/-}$ mice with $HDAC6^{-/-}$ T cells. However, ablation of HDAC6 in T cells alone was not sufficient to prevent CIPN.

Conclusions: Our results demonstrated that inhibition of HDAC6 during chemotherapy prevents CIPN in a T-cell-dependent manner. Our findings

strengthen the rationale for using HDAC6 inhibitors like ACY-1215 to not only improve cancer therapy but also prevent CIPN.

Acknowledgements: This study was supported by the National Institute of Neurological Disorders and Stroke of the National Institutes of Health (R01 CA208371 and CA227064) and by Regenacy Pharmaceuticals.

Sphingosine-1-phosphate receptor 1 in exercise-induced tumor vascular remodeling

Enrica Marmonti and Keri Schadler

Division of Pediatrics, Center for Energy Balance in Cancer Prevention and Survivorship, The University of Texas MD Anderson Cancer Center, Houston, TX.

Background: High-dose chemotherapy is the standard of care for most solid tumors, including Ewing sarcoma (ES), an aggressive bone and soft tissue sarcoma. High doses of chemotherapy are needed in part because of inefficient drug delivery to the tumor due to a hyperpermeable tumor vasculature. Improving tumor vessel function may deliver more chemotherapy and thus increase drug efficacy. One means of inducing tumor vascular normalization may be increasing shear stress. Shear stress is the physiological force created by blood flow important for maintaining vessel functionality. We found that increasing shear stress via moderate exercise caused tumor vascular normalization, increasing functionality and chemotherapy delivery in ES-bearing mice. However, the molecular mechanisms regulating tumor vasculature response to exercise are unclear. Vessel permeability is partly controlled by the G-protein-coupled receptor sphinosine-1-phsosphate receptor 1 (S1PR1) in endothelial cells (ECs). S1PR1 expression is induced by shear stress in a ligand-independent manner. We hypothesize that moderate exercise corrects tumor vessel hyperpermeability and thus improves chemotherapy delivery by increasing S1PR1 signaling. We

further hypothesize that S1PR1 on ES endothelium is necessary for enhanced tumor vascular function and chemotherapy delivery. In this study, we used treatment with a pharmacological inhibitor (FTY720) and activator (SEW2871) of S1PR1 receptor or exercise to determine whether modulation of this pathway is a clinically relevant means of enhancing chemotherapeutic efficacy in ES mouse models.

Experimental Design: TC71 and A673 ES cells from tumor-bearing mice were treated with 1) doxorubicin and/or exercise, 2) doxorubicin and/or FTY720 (antagonist of S1PR1), or 3) doxorubicin and/or SEW2871 (agonist of S1PR1). Tumor growth, vascular architecture, and permeability to high-molecular weight dextran were characterized. FTY720 antagonism and SEW2871 agonism of S1PR1 were confirmed using Western blot analysis of downstream mediators of S1PR1 signaling (S1PR1, pERK1/2, and pAKT) in lung and tumor ECs.

Results: Moderate aerobic exercise markedly reduced vascular leakiness and improved chemotherapy efficacy in TC71 tumor-bearing mice. Immunohistochemical analysis demonstrated that exercise increased the expression of S1PR1 in tumor ECs. In A673 and TC71 ES-bearing animals, FTY720 administration inhibited S1PR1 expression in tumor and lung ECs. Also, the ratio of downstream S1PR1 mediators $pERK_{1/2}/ERK_{1/2}$ and $pAkt_1/Akt_1$ was reduced in lung homogenates, demonstrating S1PR1 signaling inhibition by FTY720. The vasculature of tumors in mice given FTY720 was characterized by

increased vascular permeability. *In vivo*, S1PR1 inhibition combined with doxorubicin increased vascular leakiness and reduced doxorubicin efficacy when compared with chemotherapy alone. In contrast, S1PR1 activation by SEW2871 administration substantially increased the ratio of $pERK_{1/2}/ERK_{1/2}$ in tumor ECs demonstrating S1PR1 signaling activation, reduced tumor vascular permeability, and increased doxorubicin efficacy.

Conclusions: Moderate aerobic exercise is a nontoxic and cost-effective adjuvant for remodeling tumor vasculature and improving the efficacy of anticancer therapies. Exercise is also a nonpharmacological activator of S1PR1 signaling on tumor endothelium. Increased expression or activation of S1PR1 on tumor endothelium may be necessary to reduce the vascular hyperpermeability of blood vessels and improve chemotherapy delivery. Further work using genetic deletion of S1PR1 in combination with exercise is needed to determine whether exercise-induced vascular remodeling is S1PR1-dependent.

MBIP promotes cell motility and metastasis in Kras/p53 mutant non-small cell lung cancer

Joshua Kapere Ochieng, Samrat Kundu, Jared Fradette, Don L. Gibbons

Department of Thoracic/Head and Neck Medical Oncology, The University of Texas MD Anderson Cancer Center, Houston, TX.

Lung cancer remains the most lethal human cancer, with significantly high morbidity and mortality rates due to metastasis. Current understanding of cancer metastasis is limited due to its largely unidentified specific molecular drivers, the complexity of the metastatic process, and its underlying mechanisms, which remain poorly understood. Non-small cell lung cancer patients have dismal survival, so effective therapeutic interventions to improve patient outcome are urgently needed. We recently employed a comprehensive *in vivo* gain-of-function screen to identify genes that are potential critical drivers of metastasis. Using this approach, we identified MAP3K12-binding inhibitory protein (MBIP), a gene capable of inducing the metastatic cascade in Kras/p53-mutant mice. MBIP is part of the Ada2a-containing complex and is essential for histone modification. In addition, it inhibits MAP3K12, thereby activating the JNK/SAPK pathway. We found that elevated MBIP expression in 393P nonmetastatic epithelial cells enhanced their ability to invade, migrate, and form invasive protrusions in three-dimensional cultures. Conversely, MBIP depletion in 344SQ mesenchymal cells not only inhibited their migratory and invasive capacity but also reduced their aggressiveness in a three-dimensional collagen Matrigel matrix. The Cancer

Genome Atlas and Oncomine data set and immunohistochemical analyses revealed a sharp increase in mRNA and protein expression corresponding with markedly elevated expression of MBIP. Although MBIP may play a pivotal role in cell motility and invasion *in vitro*, little is known about its biology in lung cancer metastasis. To that end, we induced MBIP overexpression or knockdown in Kras/p53-expressing cells in mice and examined tumorigenesis and lung metastasis in the mice relative to those in controls. We found that MBIP-overexpressing (393P) mice exhibited markedly greater lung tumor burdens and growth and numbers of metastatic nodules than did control mice. Moreover, when we injected MBIP-knockdown cells (344SQ) into mice, we noted considerably fewer metastatic nodules than in the controls. To gain global insight into the impact of MBIP on signaling pathways in metastatic non-small cell lung cancer, we employed Ingenuity Pathway Analysis coupled with microRNA database searches (TargetScan, miRWalk, and PicTar) to survey MBIP. Ingenuity Pathway Analysis identified signaling nodules involved in the MAPK pathway, whereas it identified the microRNA miR-183, which is known to regulate Ezrin (a cytoskeletal protein important for invadopodia formation), as an MBIP target. We confirmed the pathway analysis results using Western blotting and immunohistochemistry, demonstrating increased levels of phosphorylated p38, Erk1/2, and Jnk in cells with elevation of MBIP expression. Also, Ezrin mRNA and phosphorylated protein levels were higher in metastatic nodules than in corresponding tumors in control mice. In addition, we observed epithelial-to-mesenchymal transition as tumors metastasized to the lungs. Taken together,

our data demonstrated that the metastatic function of MBIP is to promote cell motility and invasion of non-small cell lung cancer by inducing epithelial-to-mesenchymal transition and activating MAPK oncogenic signaling.

PD-L1 checkpoint blockade in combination with MEK inhibition reduces lung cancer metastasis

David H. Peng[1], Bertha Leticia Rodriguez[1], Laura Gibson[1], Jared Fradette[1], Limo Chen[1], Teresa Manzo[2], Ningping Feng[2], Rosalba Minelli[2], Alessandro Carugo[2], Chris Bristow[2], Jeff Kovacs[2], Tim Heffernan[2], Don Gibbons[1]

[1]Department of Thoracic/Head and Neck Medical Oncology, The University of Texas MD Anderson Cancer Center, Houston, TX; [2]Center for Co-Clinical Trials, The University of Texas MD Anderson Cancer Center, Houston, TX.

Non-small cell lung cancer (NSCLC) is the leading cause of cancer-related deaths due to late-stage disease presentation, metastasis, and resistance to conventional treatment, suggesting a need for targeted therapies. About 30% of patients with lung adenocarcinoma possess an activating KRAS mutation, and pharmacological drugs that can specifically and effectively target this oncogenic protein are lacking. Although mitogen-activated protein kinase kinase (MEK) is a canonical downstream effector of activated mutant KRAS in the mitogen-activated protein kinase (MAPK) signaling pathway, MEK inhibitors have failed to yield clinical benefit for KRAS-mutant cancers. To investigate this, we evaluated *in vivo* hairpin screens, proteomic profiles, and large patient data sets and observed an inverse correlation between MEK inhibitor sensitivity and a Zeb1-dependent epithelial-to-mesenchymal transition (EMT) state in tumors. Additionally, previous work by our group demonstrated that EMT contributes to an immunosuppressive tumor microenvironment through increased PD-L1

expression. Herein we show that treatment of lung cancer cells with an MEK inhibitor upregulates Zeb1 and PD-L1 whereas conversely, PD-L1 immune checkpoint blockade downregulates Zeb1 and enhances MAPK signaling. Combination of the MEK inhibitor with PD-L1 blockade had a synergistic effect in reducing drug-resistant lung tumor growth and metastasis, including MEK inhibitor-induced metastasis. The decrease in tumor growth and metastasis resulting from the dual treatment correlated with a synergistic increase in total and memory/effector CD8+ T-cell infiltration followed by a synergistic decrease in naïve and exhausted CD8+ T-cell populations. In future studies, researchers will aim to perform coclinical trials of the combination therapy using autochthonous murine models and further delineate the mechanism behind T-cell recruitment and activation by the combinatorial treatment.

The role of activated Beta-catenin/Wnt signaling in the progression of castration resistance of prostate cancer in bone

Justin M. Roberts, Estefania Labanca, Peter Shepherd, Jun Yang, Michael W. Starbuck, Nora M. Navone

Department of Genitourinary Medical Oncology, The University of Texas MD Anderson Cancer Center, Houston, TX.

Bone metastases typically develop in patients with advanced prostate cancer (PCa). These metastases are osteoblastic (bone-forming) and constitute the main cause of morbidity and mortality. Androgen deprivation is commonly used to treat bone metastases of PCa, but responses to such therapy are short, and the disease eventually progresses to a castration-resistant form. Bone is the primary site of castration-resistant PCa (CRPC) progression. Further development of therapies for bone metastases of PCa requires an understanding of the mechanisms underlying the growth of CRPC in bone. Clinical and laboratory-based investigations have implicated a role for PCa cell-bone cell interaction in the growth of PCa and have demonstrated that osteoblasts produce factors that favor the growth and survival of PCa cells. Collectively, these observations strongly suggest that PCa cells interact with osteoblasts and that this interaction contributes to the growth of PCa in bone. In a recent study, 18% of patients with metastatic CRPC harbored alterations in the Wnt canonical pathway, including hotspot mutations of β-catenin (β-cat), the molecular node of the Wnt canonical pathway that leads to pathway activation. This report is in

agreement with previous published reports of nuclear β-cat accumulation, an indirect measure of Wnt canonical pathway activation, in 20-40% of advanced PCas. We previously reported that an MDA-PCa-118b patient-derived xenograft developed in our laboratory harbors a β-cat mutation (D32G) and has an activated Wnt canonical pathway. MDA-PCa-118b induces an osteoblastic reaction when it is implanted in the bone of mice *in vivo. In vitro*, MDA-PCa-118b induces osteoblast proliferation in coculture. In contrast, the PCa cell line PC3 induces osteolytic lesions *in vivo* and *in vitro* and inhibits osteoblast proliferation in coculture. Strikingly, expression of β-cat mutated at D32G in PC3 cells reverses the osteoblast-inhibitory effect of PC3 cells, resulting in increased proliferation of osteoblasts when grown in coculture. We therefore hypothesize that β-cat/Wnt signaling in PCa cells mediates the PCa-bone interaction that favors PCa growth in bone. Our future studies will focus on the importance of β-cat mutations recently identified in patients with metastatic CRPC and determining whether these mutations also result in an osteoblastic phenotype, which in turn supports growth of PCa in bone. Additionally, we are screening our collection of PCa patient-derived xenograft lines for increased β-cat expression using immunohistochemistry and will sequence DNA from patient-derived xenograft lines that demonstrate increased nuclear β-cat expression to test them for activating mutations of β-cat. Our aim is to gain insight into the mechanism of the paracrine interaction between PCa cells and bone that supports the growth of PCa bone lesions, with the ultimate goal of developing therapies to block these

interactions and reduce the morbidity and mortality associated with metastatic disease.

Comprehensive molecular characterization of the Hippo signaling pathway in cancer

Yumeng Wang[1,2], Xiaoyan Xu[2,3], Dejan Maglic[4-6], Michael T. Dill[4-6], Kamalika Mojumdar[2], Kwok-Shing Ng[7], Kang Jin Jeong[7], Yiu-Huen Tsang[8], Chad J. Creighton[8,9], Gordon B. Mills[7], Fernando Camargo[4-6], Han Liang[2,7]

[1]Graduate Program in Quantitative and Computational Biosciences, Baylor College of Medicine, Houston, TX; [2]Department of Bioinformatics and Computational Biology, The University of Texas MD Anderson Cancer Center, Houston, TX; [3]Department of Pathophysiology, College of Basic Medicine Science, China Medical University, Shenyang, Liaoning Province, China; [4]Stem Cell Program, Boston Children's Hospital, Boston, MA; [5]Department of Stem Cell and Regenerative Biology, Harvard University, Cambridge, MA; [6]Harvard Stem Cell Institute, Boston, MA; [7]Department of Systems Biology, The University of Texas MD Anderson Cancer Center, Houston, TX; [8]Department of Human Genetics, Baylor College of Medicine, Houston, TX; [9]Duncan Cancer Center-Biostatistics, Baylor College of Medicine, Houston, TX.

Hippo signaling moderates cell proliferation and differentiation and is recognized as a key tumor suppressor pathway in cancer. We performed comprehensive molecular characterization of 19 Hippo core genes in 9125 tumor samples across 33 cancer types using multidimensional “omic” data from The Cancer Genome Atlas. We systematically identified somatic drivers among Hippo genes and the related microRNA regulators, including experimentally characterized YAP and

TAZ mutation effects and miR-590 and miR-200a regulation for TAZ. Hippo pathway activity is best characterized by a YAP/TAZ transcriptional target signature of 22 genes with robust prognostic power across cancer types that is correlated with epithelial-to-mesenchymal transition, DNA damage, and infiltrating immune cell composition. Our elastic-net integrated modeling further revealed cancer type-specific pathway regulators and associated cancer drivers. Our results also highlighted the importance of Hippo signaling in squamous cell cancers, characterized by frequent amplification of YAP/TAZ, high expression heterogeneity, and significant prognostic patterns. This study provides a systematic view of Hippo molecular aberrations in different tumor contexts and lays the foundation for developing Hippo-targeted therapeutic strategies.

Phosphatidylserine (PS) externalization facilitates membrane vesiculation through decreasing membrane stiffness

Hongyin Wang, Joseph Lorent, Lakshmi Ganesan, Barbar Diaz-Rohrer, Kandice Levental, Eric Malmberg, Ilya Levental

Department of Integrative Biology and Pharmacology, McGovern Medical School at The University of Texas Health Science Center at Houston, Houston, TX.

Extracellular vesicles (EVs), including exosomes and microvesicles, play critical roles in intercellular communication by exchanging proteins, lipids, and genetic materials between cells. However, the origin and biogenesis of these vesicles remain unclear. Authors have noted that almost all EVs present the anionic membrane lipid phosphatidylserine (PS) on their outer leaflets, which is in opposition to their cells of origin, which almost exclusively retain PS in the cytoplasmic leaflet. The “scrambling” of PS from the inner to the outer leaflet of the bilayer is facilitated by the lipid channel Ano6. This process of lipid scrambling is implicated in a variety of physiological contexts, including apoptotic cell removal, bone mineralization, viral infection, myoblast fusion, erythrocyte clearance, synaptic pruning, and blood coagulation. However, the biophysical role of PS externalization in the formation of extracellular vesicles remains a mystery. Using micrometer-sized giant plasma membrane vesicles produced by membrane blebbing from mouse B cells (BaF3), we studied the role of PS externalization in membrane vesiculation. We first found that a scramblase (i.e., Ano6)-knockout BaF3 cell line was deficient in producing large vesicles when

compared with the wild-type cell line, whereas Ano6-retransformed knockouts rescued the phenotype, indicating that PS externalization is necessary for membrane budding. Importantly, using fluorescence lifetime imaging microscopy with a reporter of lipid packing (Di4), we found that PS exposure led to a decrease in plasma membrane packing, potentially making the membrane softer for bending and thus facilitating membrane budding. To confirm this, we artificially decreased the lipid order on the plasma membrane by increasing the incubation temperature or treating cells with methyl-β-cyclodextrin. Under all conditions that reduced membrane stiffness, the PS externalization-deficient Ano6-knockout cell line efficiently produced large vesicles, confirming the crucial role of membrane stiffness in cell vesiculation. In summary, our study uncovered that membrane softening due to lipid scrambling was the major biophysical mechanism by which PS externalization regulated membrane vesiculation. Notably, membrane budding was controlled only by PS exposure, not by the overall PS level.